Multi-lab study on the pure-gas permeation of commercial polysulfone (PSf) membranes: measurement standards and best practices

Katherine Mizrahi Rodriguez[1], Wan-Ni Wu[2], Taliehsadat Alebrahim[3], Yiming Cao[4], Benny D. Freeman[5], Daniel Harrigan[6], Mayank Jhalaria[7], Adam Kratochvil[8], Sanat Kumar[7], Won Hee Lee[9], Young Moo Lee[9], Haiqing Lin[3], Julian M. Richardson[5], Qilei Song[10], Benjamin Sundell[6], Raymond Thür[11], Ivo Vankelecom[11], Anqi Wang[10], Lina Wang[4], Catherine Wiscount[8], and Zachary P. Smith[2]*

**Corresponding author: zpsmith@mit.edu*.

[1]Department of Materials Science and Engineering, Massachusetts Institute of Technology, 77 Massachusetts Avenue, Cambridge, MA 02139, USA.

[2]Department of Chemical Engineering, Massachusetts Institute of Technology, 77 Massachusetts Avenue, Cambridge, MA 02139, USA.

[3]Department of Chemical and Biological Engineering, University at Buffalo, The State University of New York, Buffalo, NY 14260, USA.

[4]Dalian Institute of Chemical Physics, Chinese Academy of Sciences, Dalian 116023, China.

[5]Department of Chemical Engineering, University of Texas at Austin, Austin, Texas, USA.

[6]Aramco Research Center − Boston, Aramco Services Company, Boston, Massachusetts 02139, USA

[7]Department of Chemical Engineering, Columbia University, New York, New York, USA.

[8]Air Products and Chemicals Inc., Allentown, Pennsylvania, USA.

[9]Department of Energy Engineering, College of Engineering, Hanyang University, Seoul 04763, Republic of Korea

[10]Barrer Centre, Department of Chemical Engineering, Imperial College London, London, UK.

[11]Membrane Technology Group, cMACS, KU Leuven, Celestijnenlaan 200f, Box 2454, 3001 Leuven, Belgium

Keywords

Gas separation membranes; standardization methods; polysulfone (PSf); interlaboratory study

Abstract

Gas-separation membranes are a critical industrial component for a low-carbon and energy-efficient future. As a result, many researchers have been testing membrane materials over the past several decades. Unfortunately, almost all membrane-based testing systems are home-built, and there are no widely accepted material standards or testing protocols in the literature, making it challenging to accurately compare experimental results. In this multi-lab study, ten independent laboratories collected high-pressure pure-gas permeation data for H_2, O_2, CH_4, and N_2 in commercial polysulfone (PSf) films. Equipment information, testing procedures, and permeation data from all labs were collected to provide (1) accepted H_2, O_2, CH_4, and N_2 permeability values at 35°C in PSf as a reference standard, (2) statistical analysis of lab-to-lab uncertainties in evaluating permeability, and (3) a list of best practices for sample preparation, equipment set-up, and permeation testing using constant-volume variable-pressure apparatuses. Results summarized in this work provide a reference standard and recommended testing protocols for pure-gas testing of membrane materials.

1. Introduction

New gas separation membrane materials continue to be developed every year (**Figure 1**). Despite the field's rapid growth, there are no widely accepted standards and best practices for testing, making it difficult to cross-validate experimental protocols and reliably compare results between labs. Despite a few recent efforts to commercialize membrane testing equipment, permeation systems are frequently home-built, resulting in protocols and calibration methods that

are different for each lab. Making this situation more complex, experimental methods and calibration details are often missing from publications. As a result, incoming membrane scientists can have a difficult time designing and calibrating new testing equipment. Given the current state of the field, experimental variability is expected, but heuristically, such variability becomes even more pronounced with increasingly complex materials chemistries (e.g., super-glassy polymers, multi-dimensional nanomaterials, and hybrid mixed-matrix membranes), which have gained traction due to their ability to outperform traditional polymer membranes [1–3]. These non-equilibrium and heterogeneous structures result in permeation data that can be highly sensitive to subtle changes in environmental conditions and experimental variables [2,4]. As the accessible permeation properties (i.e., permeability and selectivity) for new materials continue to expand and the membrane science community continues to grow, the need to establish community-wide standards becomes more urgent.

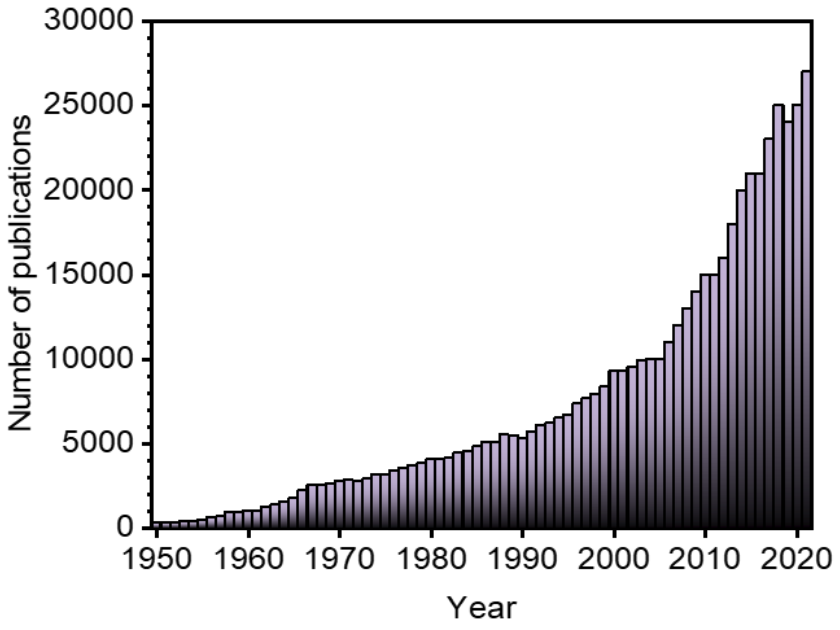

Figure 1. Growth in the number of publications related to gas separation membranes. Data were collected through a search in Scifinder® using "Gas Separation Membrane(s)" as keywords.

Reproducibility matters in all areas of research [5–8]. Researchers in the fields of biology and social sciences have spearheaded efforts to build awareness around reproducibility [9–11], and many standardization studies have been developed broadly within the scientific community. In terms of adsorbent materials, Sholl and coworkers have evaluated the variability in metal–organic framework (MOF) syntheses [12] as well as considering variability in MOF sorption isotherms [13] for thousands of reported data, resulting in a short but helpful list of recommendations to encourage researchers to make their science more reproducible [14]. In the separations community, studies to standardize testing of zeolite adsorption [15] and osmotically driven processes [16] have been well-received, and recommendations to bridge the gap between academic and industrial evaluation of mixed-gas separation have been recently reported [17]. Aiming to further these efforts, in 2019, a report by the National Academies of Sciences, Engineering, and Medicine encouraged the membrane community to develop standards for transport testing systems [18].

This study was designed to establish permeation testing protocols for the membrane community. A detailed overview of experimental techniques used for permeation testing can be found elsewhere [19]. To the best of our knowledge, the only published standard on gas permeability came from the American Society for Testing and Materials (ASTM, D1434) in 1982. This study determined gas permeability in plastic films and film sheeting, and included an interlaboratory analysis from 1965 using polyethylene, polypropylene, and a commercial polyester (Mylar 100A and 65HS) [20]. These polymers are usually semi-crystalline polymers and therefore not as frequently used for gas separation applications. Unfortunately, when considering commercial samples of more commonly used glassy or rubbery materials, there are no widely accepted standards for pure-gas permeation, and correspondingly, there are no surveys of methods that describe experimental protocols. In response to these missing pieces of information, this study

provides: (1) a standard measurement protocol for membrane-based permeation testing across multiple laboratories and (2) a reference standard for groups to use when evaluating a new constant-volume variable-pressure permeation system. We report H_2, O_2, N_2, and CH_4 permeation for a commercial PSf film at 10 bar, 15 bar, and 20 bar, collected from ten different labs in the membrane community. Detailed equipment information, testing procedures, and as-submitted data were used to define accepted values for permeabilities, time lags, and diffusion coefficients. Finally, recommended practices for minimizing variation in permeation testing are provided.

2. Theory and methods

Gas transport in a polymer film is frequently described using the sorption–diffusion model [21]:

$$P = D \times S \tag{1}$$

where P is the permeability or the pressure- and thickness- normalized flux through a film in units of barrer (10^{-10} cm^3_{STP} cm^{-3}_{pol} cm^2 $cmHg^{-1}$ s^{-1}), D is the concentration-averaged diffusion coefficient (cm^2 s^{-1}), and S is the sorption coefficient (cm^3_{STP} cm^{-3}_{pol} $cmHg^{-1}$).

Sorption coefficients can be obtained directly from sorption experiments or indirectly by the time-lag method. In the former case, sorption isotherms of glassy polymers such as PSf are often interpreted using the dual-mode sorption (DMS) model [22]:

$$\mathrm{C} = k_D p + \frac{C'_H b p}{1 + b p} \tag{2}$$

where C is the concentration of gas in the polymer (cm^3_{STP} cm^{-3}_{pol}), p is the equilibrium pressure (cmHg), C'_H is the Langmuir capacity (cm^3_{STP} cm^{-3}_{pol}), k_D is the Henry's law constant (cm^3_{STP} cm^{-3}_{pol} $cmHg^{-1}$), and b is the Langmuir affinity constant ($cmHg^{-1}$). In a typical sorption experiment, the sorption coefficient is calculated by dividing the concentration of gas sorbed in

the polymer by pressure (**Eq. 3**). Using the DMS model, permeability can be written as **Eq. 4** [23]. A generalized equation with this functional form and three parameters (x, y, and z) was used to fit the permeation data gathered in this study. The fitted parameters are simply used to match the expected mathematical form of the transport relationship. Therefore, these parameters should not be ascribed any physical meaning, but instead, should be viewed as best-fit parameters for reported permeabilities.

$$S = \frac{C}{p} = k_D + \frac{C_H' b}{1 + bp} \tag{3}$$

$$P = D \times \left(k_D + \frac{C_H' b}{1 + bp} \right) = x + \frac{yz}{1 + zp} \tag{4}$$

The diffusion coefficients can be calculated by monitoring transport kinetics and solving Fick's second law with appropriate initial and boundary conditions [24]. Under the assumption of concentration-averaged diffusion coefficients, time-lag analysis [25,26] or kinetic sorption experiments are frequently used to determine diffusion coefficients [24,27]. For time-lag analysis, one-dimensional diffusion equations are solved assuming isotropic membrane materials [28]. In this case, the total amount of gas that flows through a flat-sheet membrane at steady-state is defined as Q_t:

$$Q_t = \frac{D C_2}{l} \times \left(t - \frac{l^2}{6D} \right) \tag{5}$$

where l is the membrane thickness (cm), t is the time (s), and D is the diffusion coefficient (cm^2 s^{-1}). For these experiments, both sides of the film are initially under vacuum, so the penetrant concentration of the entire system is $C = 0$ at $t = 0$. Pressure is applied instantaneously at the upstream face of the film, and assuming rapid sorption at the surface, a concentration of C_2 is

maintained just inside of the upstream film boundary for the entirety of the experiment. Conversely, the downstream is maintained under vacuum for the entirety of the experiment, requiring a concentration of $C = 0$ at this interface. After the permeation test, Q_t is plotted against time, and according to **Eq. 5**, the x-intercept is defined as the time-lag (θ), where the diffusion coefficient is defined as [28]:

$$D = \frac{l^2}{6\theta} \tag{6}$$

2.1. Constant-volume variable-pressure testing apparatus

Pure-gas permeation testing is often performed using either a constant-volume variable-pressure apparatus or a constant-pressure variable-volume apparatus. The latter is more typically used for highly permeable films or composite membranes, or for evaluation of gas mixtures [19]. Constant-volume variable-pressure systems require the evaluation of flux into a known volume. As a result, this method can be used for (1) permeability testing in materials with very low penetrant flux (e.g., PSf) and (2) collection of the time-lag diffusion data. This study focuses on standardization for pure-gas testing in a constant-volume variable-pressure apparatus.

A schematic of a generalized constant-volume variable pressure system is shown in **Figure 2.** In a typical permeation test, the entire system and sample is evacuated to remove residual gases or moisture. The temperature is controlled by a water or air bath. The permeation cell, typically an in-line stainless steel filter holder, is sealed with two o-rings that contain the membrane sample. Next, the upstream is filled with the gas of interest at a set upstream pressure monitored by the upstream pressure transducer (P_u). To begin a test, the upstream and downstream volumes are isolated with a valve and gas is pressurized at the upstream face of the sample. The gas permeates through the film and accumulates in the downstream volumes (V_1 or V_2). The downstream pressure

must be significantly lower than the upstream pressure to maintain a near constant pressure differential across the film. A downstream pressure transducer (P_d) is used to monitor the pressure rise in the downstream volume.

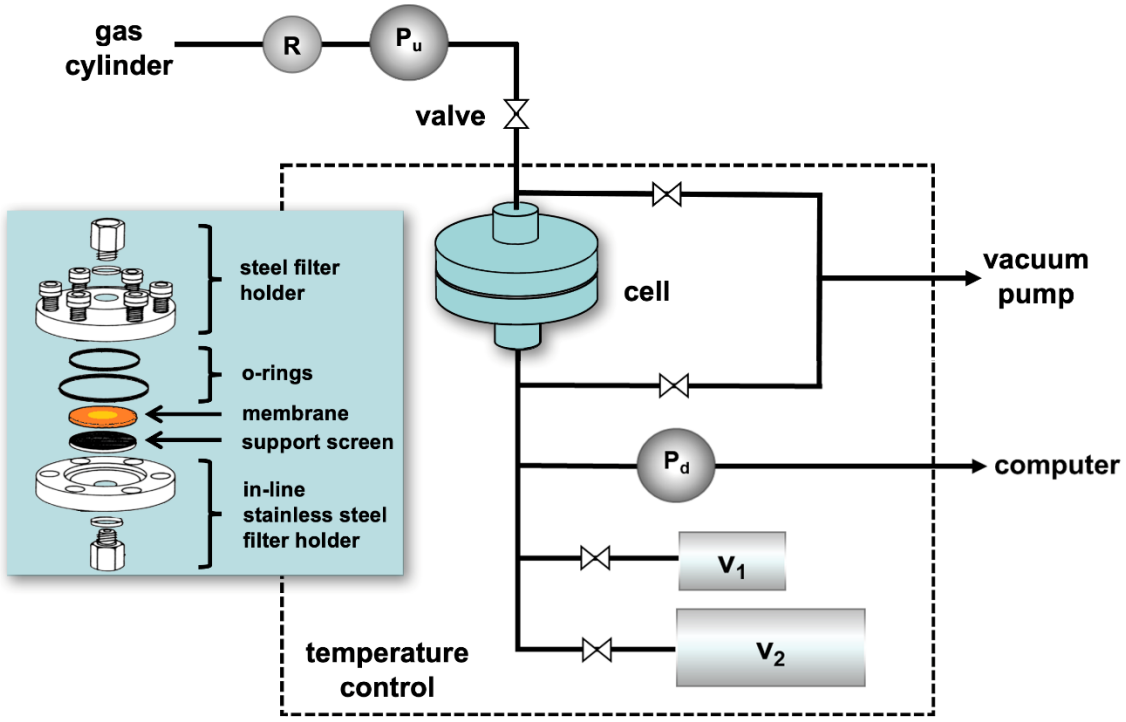

Figure 2. Generalized schematic of a constant-volume variable-pressure permeation system, where R is the pressure regulator, P_d and P_u are the downstream and upstream pressure transducers, and V_1 and V_2 are downstream volumes. This image was adapted from reference [19].

Pure-gas permeability, P, is calculated according to **Eq. 7**:

$$P = \frac{l\,V_d}{(p_2 - p_1)\,A\,R\,T} \times \left[\left(\frac{dp_1}{dt}\right)_{ss} - \left(\frac{dp_1}{dt}\right)_{leak}\right] \tag{7}$$

where p_2 is the average upstream pressure (cmHg), p_1 is the average downstream pressure (cmHg), V_d is the volume in the downstream (cm^3), $\left(\frac{dp_1}{dt}\right)_{ss}$ is the steady state pressure rise in the downstream (cmHg s^{-1}), $\left(\frac{dp_1}{dt}\right)_{leak}$ is the leak rate (cmHg s^{-1}), and A is the cross-sectional area of

the sample exposed to the permeating gas (cm^2). The term T is the absolute temperature (K), and R is the ideal gas constant (0.278 cmHg cm^3 cm^{-3}_{STP} K^{-1}). Adjustments for fugacity are commonly considered to calculate permeability for condensable gases at elevated pressures or temperatures.

2.2. Multi-lab experimental procedure and materials

2.2.1. Materials: PSf was identified as a suitable reference material due to its commercial availability as a film [29,30], moderately low aging susceptibility compared to other bulk glassy polymer films [31], and absence of crosslinking agents or additives in its casting, as is common with rubbery materials such as PDMS [32].

2.2.2. Multi-lab study protocol: Ten laboratories participated in this study, including industrial and academic participants. The testing capabilities and specific configurations of the systems used by each participant ranged in style from home-built to manual or automatic systems. All laboratories were required to:

(1) Purchase commercial PSf films from Goodfellow & Co. (SU341025).

(2) Prepare three individual samples for testing and test H_2, O_2, N_2, and CH_4 at 10 bar, 15 bar, and 20 bar at 35 °C using standard testing protocols for each participating lab.

(3) Analyze the data and submit the results using the Word and Excel templates shown in **Appendix 1** of the Supplementary Information (SI).

Since permeation tests may be carried out with different apparatus configurations, each lab was asked to provide a detailed experimental procedure (cf. **Appendix 4** of the SI) and detailed information on testing equipment, including the temperature control (i.e., air or water heated systems), type of film support (i.e., aluminum tape, epoxy, etc.), leak rate, testing times, etc. This data is summarized in **Tables S3–7** and all data are reported anonymously (e.g., Lab 1).

This study focuses on establishing a literature reference material with permeabilities and uncertainties expected from identical samples tested in different laboratories and using non-plasticizing gases. Similar work for other testing instrumentation (e.g., variable-volume constant-pressure testing equipment, mixed-gas permeation, and pure- and mixed-gas sorption) or other gas penetrants (e.g., CO_2) are of high interest but beyond the scope of this study. Commercial films were intentionally selected to minimize sample-to-sample variability associated with synthetic procedures, casting protocols, or treatment conditions. In this way, we aim to evaluate only variability in testing and not variability in sample synthesis and preparation. Of course, reproducibility in sample synthesis and preparation is critical for methods development, as others have reported for materials such as MOFs [12]. Such considerations would be of great interest to the membrane community for future studies as well.

2.2.3. Self-reported data: Participants submitted permeation data for three separate PSf films tested at 10 bar, 15 bar, and 20 bar. Due to limited experimental capabilities, some labs only provided data at lower pressures or for a subset of gases. For Lab 6, three sets of data were provided in duplicate. Therefore, the results are reported as averages of as-submitted values without standard deviations (SDs). If accessible, researchers provided time-lag values for films tested at 10 bar. Diffusion coefficients were calculated using the submitted time-lag values and self-reported thicknesses. When possible, permeation, time-lag, and diffusion coefficients are reported as the average of three measurements including SDs.

2.2.4. Statistical analysis, fitting, and data re-calculation: Box and whisker plots were generated for the self-reported permeation and time-lag data. The interquartile range was defined as the difference between the first quartile (Q1) and the third quartile (Q3), which represent the 25^{th} and 75^{th} percentile of the dataset [33]. All box and whisker plots include the mean and median, narrow

colored whiskers denoting one standard deviation from the mean, and wide black whiskers representing two standard deviations from the mean (i.e., the 95% confidence interval (CI)).

To estimate the contribution of human error associated with transport rate calculations, the permeability and time-lag values were manually re-calculated by a third party at MIT using the raw data provided by each lab (cf. **Appendix 3** of the SI). Additionally, **Eq. 4** was used to develop a consensus set of permeation data among the labs for PSf permeability over the range of pressures considered (i.e., 10–20 bar). Parameters x, y, and z were obtained by fitting the self-reported permeabilities to **Eq. 4**. The nonlinear optimization was run in MATLAB using the following objective function:

$$(\mathrm{x},\mathrm{y},\mathrm{z}) = \arg\min \sum_{p=10,15,20} \sqrt{\frac{\sum_i \left(x + \frac{yz}{1+zp} - P_{expt,i}\right)^2}{N}}\Bigg|_p \tag{8}$$

where N is the number of sample points at the given pressure p, and $P_{expt,i}$ is the self-reported permeability. The uncertainties in the consensus permeability values were calculated for each pressure using **Eq. 9**:

$$\sigma = \sqrt{\frac{\sum_i (x_i - y_i)^2}{N}} \tag{9}$$

where x_i is the experimental permeability, y_i is the permeability determined from **Eq. 4** using the best fit parameters, and N is the total number of data points at each of the pressures considered.

The normality of the data was confirmed using a Shapiro–Wilk test, where a p value greater than 0.05 indicates a normal distribution [33]. Test statistics for the H_2, O_2, N_2 and CH_4 datasets at each pressure are shown in **Table S1** of the SI. Co-dependencies between permeability and parameters such as thickness, area, temperature, leak rate, pressure transport rate, and hold times

were evaluated by extracting R^2 values. R^2 values near zero indicate minimal dependencies (cf. **Appendix 2** of the SI). Z-scores were calculated according to **Eq. 10** to provide a normalized spread of the data.

$$z = \frac{x - \mu}{\sigma_x} \tag{10}$$

where x is the observed value of permeability or selectivity at a given pressure, μ is the average value, and σ_x is the standard deviation.

3. Results and Discussion

3.1. Permeability data: Self-reported H_2, O_2, N_2 and CH_4 permeabilities tested at approximately 10 bar, 15 bar, and 20 bar are shown in **Figure 3** and **Table 1**. Interestingly, the reported standard deviations varied widely from lab to lab, indicating significant variability from test to test using the same pieces of equipment. At 10 bar, for instance, the standard deviations ranged from 1.1% to 13.6% for H_2, 1.6% to 6.7% for O_2, 1.8% to 16.6% for N_2 and 3.2% to 7.1% for CH_4. These variations indicate that testing conditions and equipment specifications can lead to significant differences in reported permeation results. When high-pressure data was provided, the O_2, N_2 and CH_4 permeabilities generally decreased with increasing pressure, consistent with the dual-mode model and represented by **Eq. 4**.

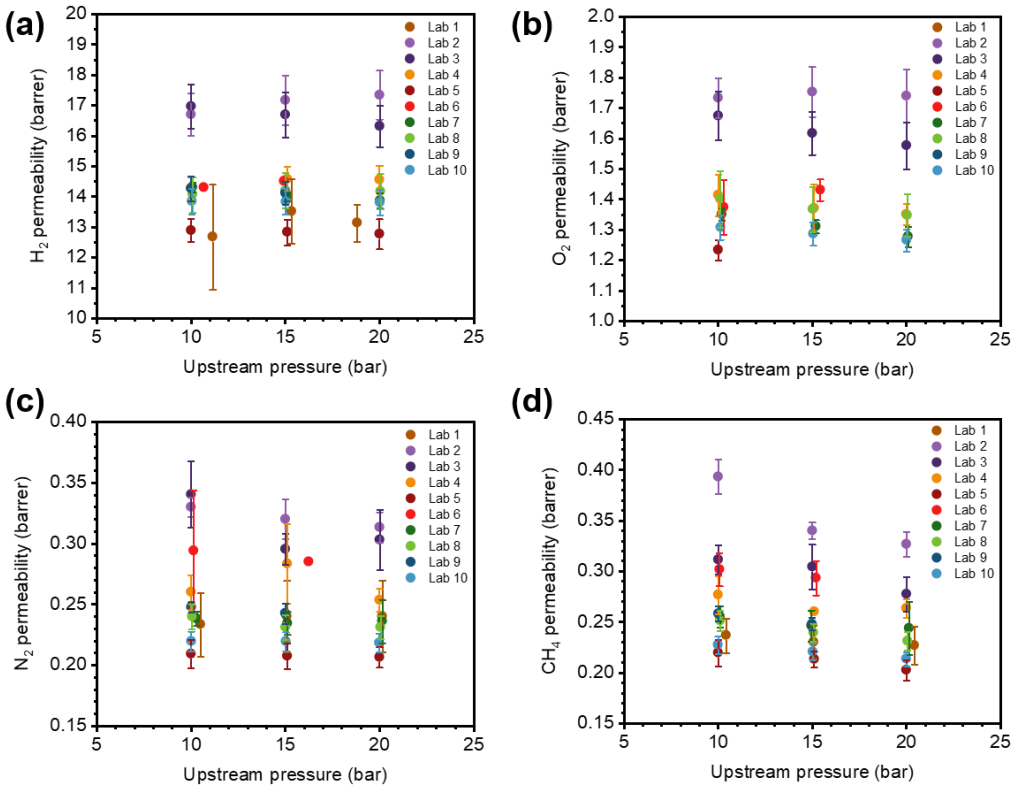

Figure 3. (a) H_2, (b) O_2, (c) N_2, and (d) CH_4 permeabilities for PSf tested at 35 °C versus the average of the self-reported upstream pressure. Error bars indicate standard deviations from three independent measurements.

Table 1. Self-reported permeabilities and associated statistical metrics for PSf tested at 35 °C.

Permeability (barrer)															
Gas		**H_2**			**O_2**			**N_2**			**CH_4**				
Pressure (bar)	**10**	**15**	**20**	**10**	**15**	**20**	**10**	**15**	**20**	**10**	**15**	**20**
Lab 1	13 ± 2	14 ± 1	13.1 ± 0.6	-	-	-	0.23 ± 0.03	0.24 ± 0.03	0.24 ± 0.03	0.24 ± 0.02	0.23 ± 0.02	0.23 ± 0.02
Lab 2	16.7 ± 0.7	17.2 ± 0.8	17.3 ± 0.8	1.73 ± 0.07	1.75 ± 0.08	1.74 ± 0.09	0.330 ± 0.008	0.32 ± 0.02	0.31 ± 0.01	0.39 ± 0.02	0.340 ± 0.008	0.33 ± 0.01
Lab 3	17.0 ± 0.7	16.7 ± 0.7	16.3 ± 0.7	1.67 ± 0.08	1.62 ± 0.07	1.58 ± 0.08	0.34 ± 0.03	0.30 ± 0.01	0.30 ± 0.02	0.31 ± 0.01	0.30 ± 0.02	0.28 ± 0.02
Lab 4	14.3 ± 0.4	14.6 ± 0.4	14.6 ± 0.5	1.41 ± 0.07	1.37 ± 0.08	1.35 ± 0.04	0.26 ± 0.01	0.28 ± 0.03	0.253 ± 0.009	0.28 ± 0.02	0.26 ± 0	0.263 ± 0.009
Lab 5	12.9 ± 0.4	12.8 ± 0.4	12.8 ± 0.5	1.23 ± 0.03	-	-	0.21 ± 0.01	0.21 ± 0.01	0.206 ± 0.008	0.21 ± 0.01	0.21 ± 0.01	0.202 ± 0.01
Lab 6	14.3	14.5	-	1.40 ± 0.09	1.43 ± 0.04	-	0.29 ± 0.05	0.29	-	0.30 ± 0.02	0.29 ± 0.02	-
Lab 7	14.3 ± 0.2	14.0 ± 0.1	13.9 ± 0.2	1.35 ± 0.02	1.31 ± 0.02	1.28 ± 0.03	0.238 ± 0.006	0.234 ± 0.009	0.24 ± 0.02	0.26 ± 0.01	0.25 ± 0.02	0.24 ± 0.03
Lab 8	14.1 ± 0.6	14.2 ± 0.6	14.2 ± 0.6	1.40 ± 0.09	1.37 ± 0.07	1.35 ± 0.07	0.24 ± 0.01	0.23 ± 0.01	0.231 ± 0.009	0.25 ± 0.01	0.239 ± 0.009	0.231 ± 0.009
Lab 9	14.3 ± 0.4	14.3 ± 0.4	-	1.41 ± 0.04	-	-	0.248 ± 0.004	0.243 ± 0.008	-	0.258 ± 0.008	0.250 ± 0.007	-
Lab 10	13.8 ± 0.4	13.8 ± 0.4	13.8 ± 0.4	1.31 ± 0.04	1.29 ± 0.04	1.26 ± 0.04	0.219 ± 0.008	0.219 ± 0.008	0.218 ± 0.008	0.227 ± 0.009	0.220 ± 0.008	0.213 ± 0.007
Mean	14.4	14.6	14.5	1.44	1.45	1.43	0.26	0.26	0.25	0.27	0.26	0.25
Median	14.3	14.2	14	1.39	1.37	1.35	0.24	0.24	0.24	0.26	0.25	0.24
SD	1.4	1.29	1.47	0.12	0.11	0.12	0.04	0.04	0.04	0.05	0.04	0.04

Box and whisker plots indicating mean, median, and standard deviation bounds for the permeability measurements are shown in **Figure 4** and **Table 1**. The majority of self-reported permeabilities for all gases were within a standard deviation from the mean (cf. **Tables 1** and **S2**), with the exception of values for Labs 1, 2, 3, and 5. This finding is consistent with statistical expectations in uncertainty. For H_2, O_2 and N_2, permeability values from Labs 2 and 3 were consistently higher than the other labs, where Lab 2 showed positive z-score values above 1.6 for every sample (cf. **Table S2**). On the other hand, for CH_4 and H_2, permeabilities from Lab 5 were often below a standard deviation from the mean. Above 10 bar, the confidence in permeabilities decreased for H_2 and O_2 due to a smaller available sample pool. Overall, the permeabilities for most gases were within two standard deviations from the mean, with the exception of one outlier for CH_4 permeability of Lab 2 at 10 bar (Z-score = 2.37). Again, these results are consistent with statistical expectations. Moreover, as shown in **Figure S1**, the spread of the data was relatively consistent from gas to gas and pressure to pressure, with most permeability values ranging from approximately one standard deviation below the mean to two standard deviations above the mean. Potential factors contributing to these deviations and the outlier data are discussed in **Section 3.3**.

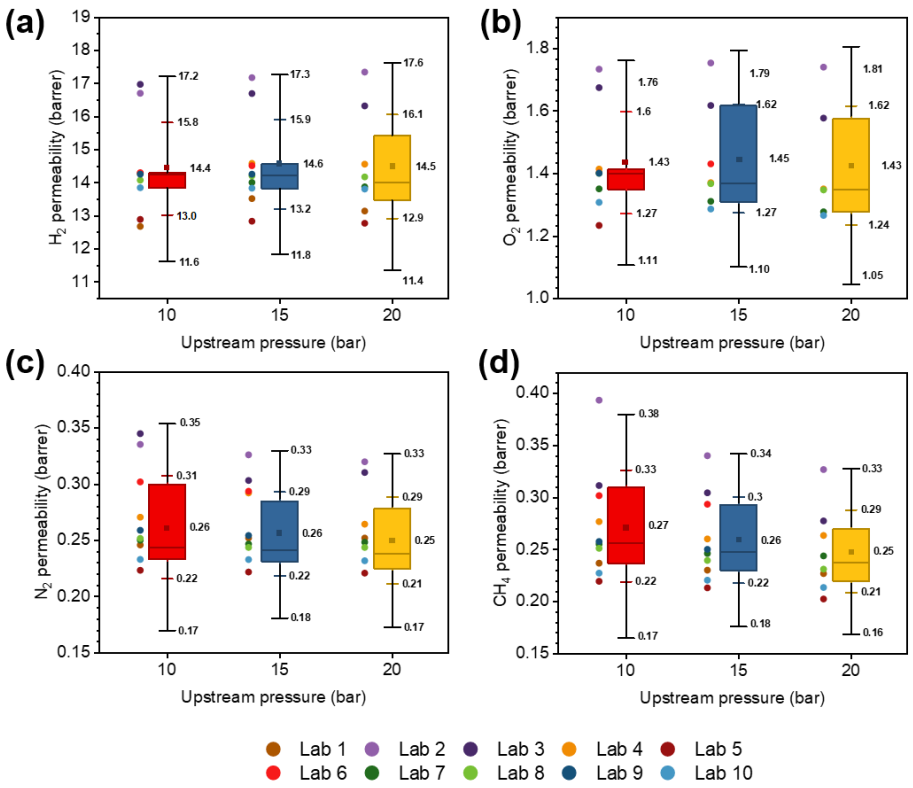

Figure 4. (a) H_2, (b) O_2, (c) N_2, and (d) CH_4 permeability box and whisker plots for PSf films tested at 35 °C. Colored whiskers and black whiskers represent one and two standard deviations from the mean, respectively. The lower and upper bounds of the box represent Q1 and Q3, respectively. The square symbol and horizontal line within the box indicate the mean and median, respectively. Colored circles indicate the average of the as submitted permeability values from each lab.

The self-reported permeabilities were also fit to **Eq. 4** to derive generalized parameters (x, y, and z) for the prediction of permeabilities at pressures between 10–20 bar. Fitting parameters are summarized in **Table S3**. As shown in **Figure 5**, the fitted curves display a sharper permeability decrease for N_2 and CH_4 compared to the other gases, as was observed for the box and whisker plots in **Figure 4**. Although this trend has very weak statistical significance, an average decrease in permeability is expected within the framework of the dual-mode model, which was used to

construct the mathematical expression for our generalized fit. Moreover, the standard deviations calculated from the fitting aligned very well with those calculated for the dataset in **Table 1** and **Figure 4** (cf. **Figure S2**), indicating that **Eq. 4** is an appropriate representation of the dataset.

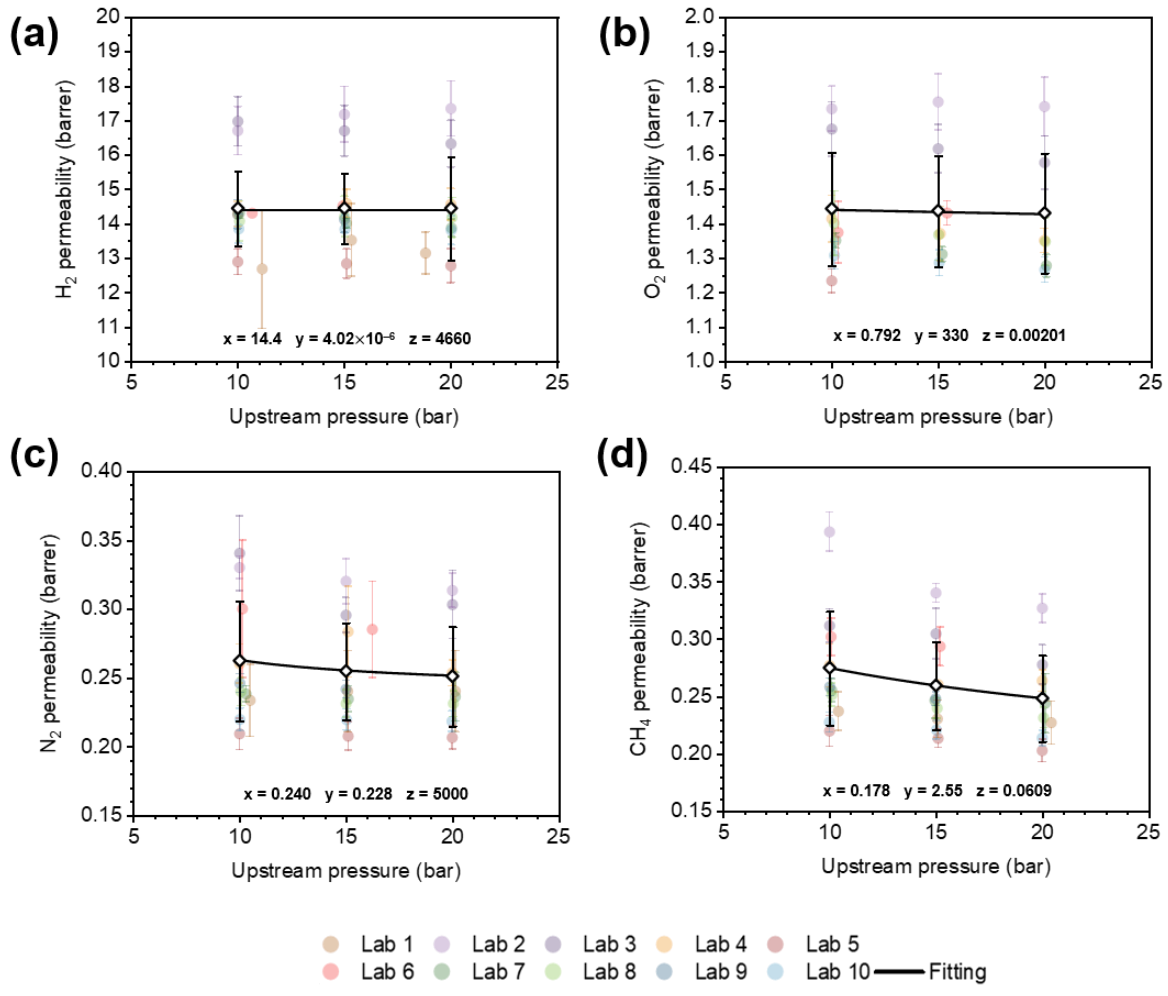

Figure 5. Fitted permeability curves and associated fitting parameters for H_2, O_2, N_2, and CH_4 permeability data tested at 35 °C.

H_2/CH_4 and O_2/N_2 selectivities were also calculated for all labs, as shown in **Figure 6** and **Table 2**. Generally, selectivity is calculated as the ratio of the permeabilities for the two gases of interest. As a result, selectivity values normalize out deviations originating from area and thickness

measurements, and, if both gases were tested using a single downstream volume, from volume calibrations as well. All labs in this study used a single downstream volume for the gas pairs evaluated, except for Lab 9. In general, selectivities showed tighter distributions than the permeability trends, suggesting that volume, areas, and thickness estimates play an important role in permeation deviations, as is further discussed in **Section 3.3**. Interestingly, while permeabilities for Labs 1, 2, 3, and 5 showed the largest deviations from the mean, the selectivities are much more consistent with the rest of the dataset, with the exception of H_2/CH_4 selectivity at 10 bar for Lab 2, which was furthest away from the dataset when compared to other labs.

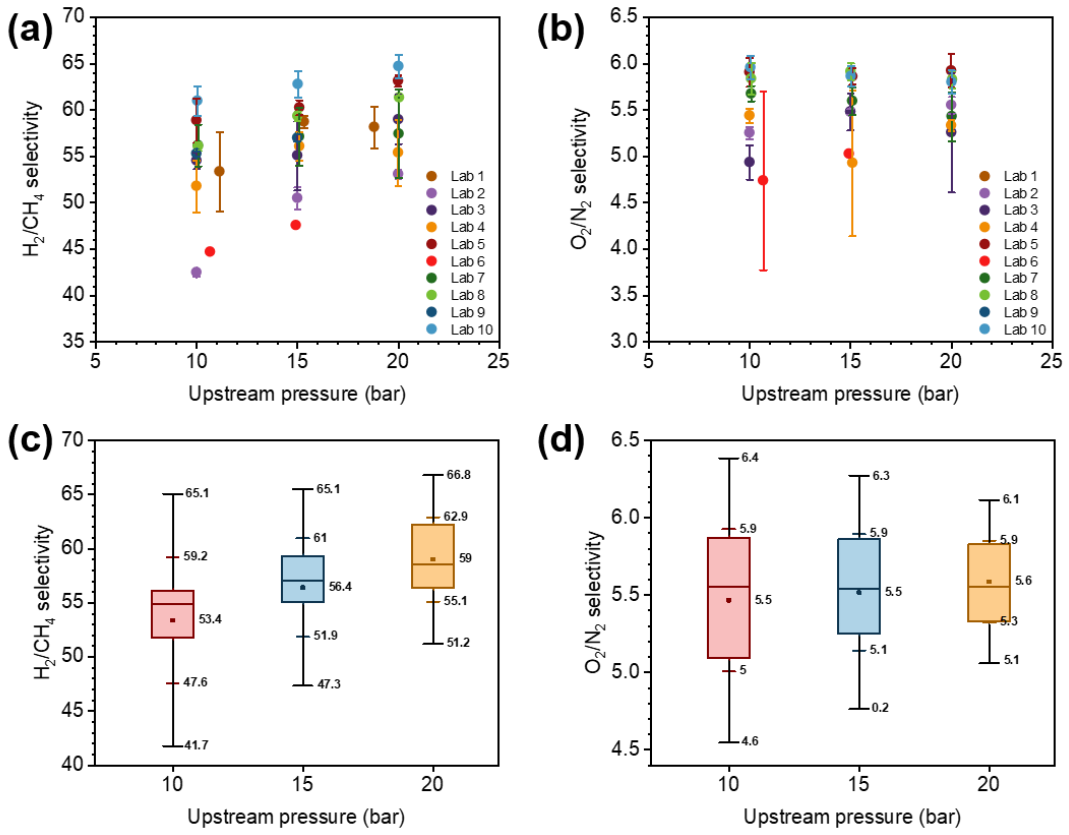

Figure 6. (a) H_2/CH_4 and (b) O_2/N_2 selectivities for PSf films tested at 35 °C. Error bars indicate standard deviations from three independent measurements. (c) H_2/CH_4 and (d) O_2/N_2 selectivity box and whisker plots for PSf films. Colored whiskers and black whiskers represent one and two

standard deviations from the mean, respectively. The lower and upper bounds of the box represent Q1 and Q3, respectively. The square symbol and horizontal line within the box indicate the mean and median, respectively.

Table 2. Self-reported selectivities and associated statistical metrics for PSf tested at 35 °C.

Selectivity						
Gas Pair	**H_2/CH_4**			**O_2/N_2**		
Pressure (bar)	**10**	**15**	**20**	**10**	**15**	**20**
Lab 1	53 ± 4	59 ± 0.6	58 ± 2	-	-	-
Lab 2	43 ± 0.4	50 ± 1	53.1 ± 0.5	5.25 ± 0.07	5.48 ± 0.03	5.55 ± 0.09
Lab 3	54.5 ± 0.9	55 ± 4	59 ± 3	4.9 ± 0.2	5.5 ± 0.2	5.3 ± 0.6
Lab 4	52 ± 3	56 ± 2	55 ± 4	5.44 ± 0.07	4.9 ± 0.8	5.33 ± 0.06
Lab 5	59 ± 2	60.2 ± 0.8	63.1 ± 0.6	5.9 ± 0.2	5.86 ± 0.09	5.9 ± 0.2
Lab 6	44.7 ± 0.3	47.5 ± 0.9	-	5 ± 1	5.0 ± 0.5	-
Lab 7	56 ± 2	57 ± 3	57 ± 5	5.67 ± 0.08	5.6 ± 0.2	5.4 ± 0.3
Lab 8	56.0 ± 0.4	59.3 ± 0.5	61.3 ± 0.2	5.8 ± 0.2	5.91 ± 0.09	5.83 ± 0.09
Lab 9	55.3 ± 0.3	57.3 ± 0.4	-	5.8 ± 0.1	-	-
Lab 10	61 ± 2	63 ± 1	65 ± 1	6.0 ± 0.1	5.9 ± 0.1	5.8 ± 0.1
Mean	53.4	56.4	59.0	5.5	5.5	5.6
Median	54.9	57.0	58.6	5.6	5.5	5.6
SD	5.5	4.3	3.6	0.43	0.35	0.24

3.2. Time lag and diffusion data: Following the same approach from the previous section, the box-plots for time-lag data are shown in **Figure 7.** Self-reported O_2, N_2 and CH_4 time-lag values are summarized in **Table 3.** Time-lag values for H_2 were not reported since the timescale for diffusion was too fast for reliable measurement within the error of the systems used in participant labs. Interestingly, there was a significantly larger variability in time-lag results compared to the permeability results. The reported time-lag values for all three gases varied widely across all labs, which resulted in imprecise time-lag measurements, which are tabulated in **Table 3**. The exact reason for such variability could be related to several factors. First, the time-lag method requires that the upstream face of the film is instantaneously pressurized to the final pressure, but there is

often a lag in this pressurization step, which increases uncertainty. There are potential methods to overcome this limitation to the time-lag solution; most notably, by considering a time-dependent and variable concentration boundary condition at the upstream of the film [24], but such an approach requires prior knowledge of sorption isotherms over the pressure range of interest and likely numerical integration, adding additional complexities to this type of analysis and limiting widespread adoption. Notably, for this study, uncertainties in the time lags were independent of the gases tested, and hence, independent of the amount of time required to perform a measurement, suggesting that the pressurization step was not the most significant source of uncertainty. For instance, standard deviations for O_2 and CH_4 time lags from study participants were approximately 20% of the mean value, despite having time lags that differed by approximately a factor of 10. Additionally, nitrogen, which had an intermediate time lag, had the highest uncertainty of the three gases considered. Another possible source of error is the amount of time that study participants waited to reach steady-state, which would influence the linear extrapolation of the time-lag curve to the x-axis, or whether or not the leak rate was subtracted from the permeability data (cf. **Figure S8**). As a final possibility, human error could result in some variability. These final considerations, which are discussed in **Section 3.3**, indicate the need for the development of standardization and best practices in the field. Despite the variation in time-lag values, O_2, N_2, and CH_4 diffusion coefficients have very similar mean and median values, indicating a Gaussian distribution with random variations in values, and no clear systematic errors for specific labs.

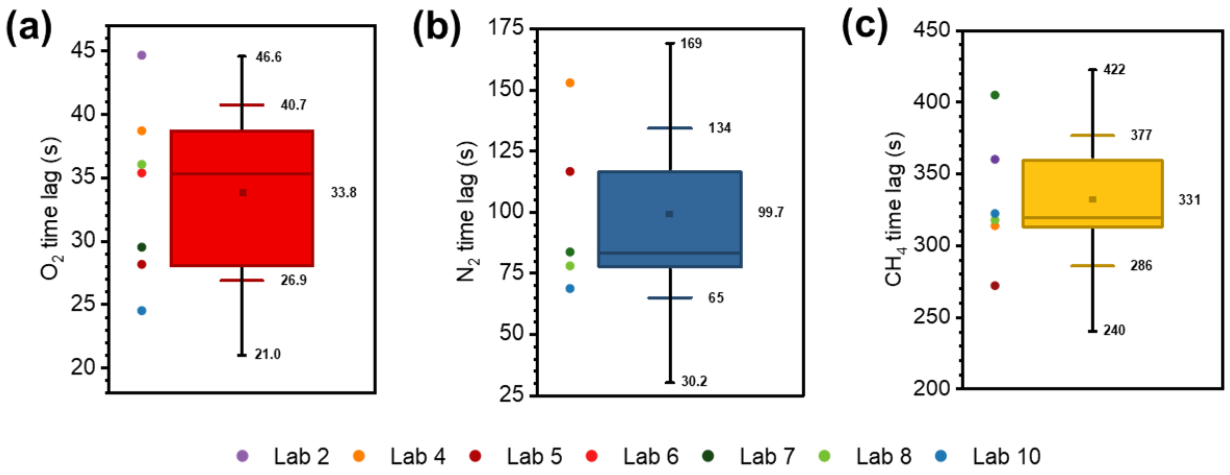

Figure 7. (a) O_2, (b) N_2, and (c) CH_4 time-lag box and whisker plots for PSf films tested at 10 bar and 35 °C. Colored whiskers and black whiskers represent one and two standard deviations from the mean, respectively. The lower and upper bounds of the box represent Q1 and Q3, respectively. The square symbol and horizontal line within the box indicate the mean and median, respectively. Colored circles represent the average of as-submitted data from each lab.

Table 3. Self-reported time lag values, calculated diffusion coefficients, and statistical metrics for PSf tested at 10 bar and 35 °C.

Metric	Time lag (s)			Diffusion coefficient (10^{-8} cm^2/s)		
Gas	**O_2**	**N_2**	**CH_4**	**O_2**	**N_2**	**CH_4**
Lab 1	-	-	-	-	-	-
Lab 2	44.6 ± 1	-	360 ± 20	2.34 ± 0.06	-	0.29 ± 0.01
Lab 3	-	-	-	-	-	-
Lab 4	39 ± 5	153 ± 9	310 ± 50	3.0 ± 0.5	0.75 ± 0.04	0.38 ± 0.07
Lab 5	28 ± 6	70 ± 20	272 ± 8	4.1 ± 0.9	1.7 ± 0.4	0.41 ± 0.04
Lab 6	35 ± 8	-	-	4.2 ± 0.6	-	-
Lab 7	29.5 ± 0.7	116 ± 8	400 ± 10	3.41 ± 0.06	0.87 ± 0.05	0.25 ± 0.01
Lab 8	40 ± 10	80 ± 20	320 ± 10	3.3 ± 0.7	1.6 ± 0.06	0.35 ± 0.02
Lab 9	-	-	-	-	-	-
Lab 10	24.4 ± 0.5	83 ± 1	320 ± 10	4.1 ± 0.2	1.2 ± 0.07	0.31 ± 0.01
Mean	33.8	99.6	331	3.5	1.2	0.33

Median	35	80.3	320	3.4	1.2	0.33
SD	7	35	50	0.7	0.4	0.06

3.3. Considerations for permeation testing protocol and best practices

Despite having tested one common commercial PSf film, self-reported permeability and time-lag values varied considerably between labs. This section summarizes common testing practices and recommended guidelines to ensure accurate permeation measurements once a film is formed. **Figure 8** illustrates a generalized workflow for permeation testing including six steps where variability can be introduced to the final permeation measurement. The rest of this section describes consensus practices and recommendations associated with each of these steps.

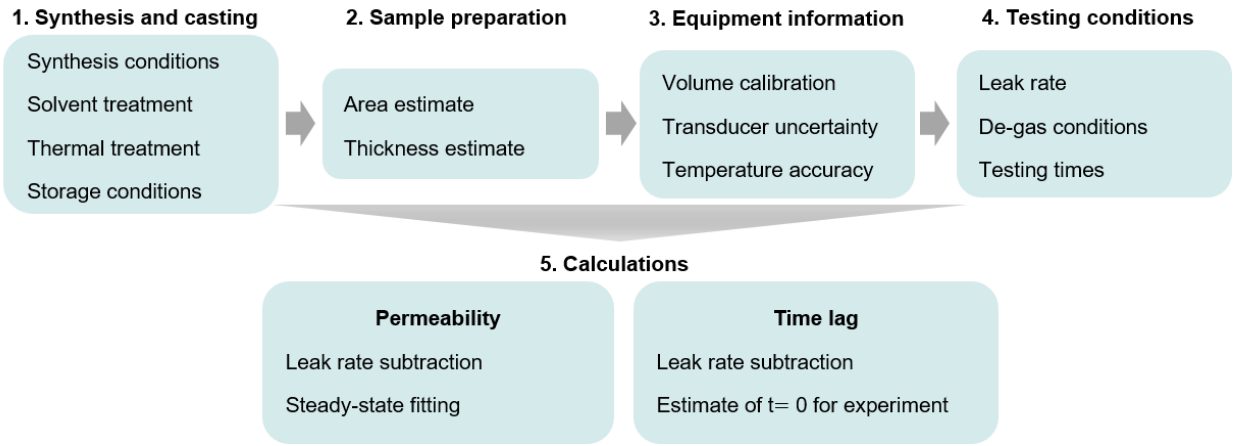

Figure 8. Generalized permeation testing workflow and relevant criteria to consider at each step.

3.3.1. Synthesis and casting

Synthesis methods [34], casting conditions (e.g., solvents [35–37]), post-casting treatments (e.g., thermal [35,38], solvent [35,39–41], or conditioning history [38]), and storage conditions [4,42] (e.g., aging time and humidity in given environments) influence transport measurements. These factors are especially important for high free volume polymers, where slight variations in

synthetic conditions, post-casting treatment, and physical aging can result in large changes in transport properties [42]. The effects of casting, treatment, and processing conditions on PSf transport properties were briefly explored by comparing the average results from this study to literature studies summarized in **Section 6** of the supplementary information [43–46]. In this study, the effects of physical aging were not considered. Labs ordered films and tested them on their independent timeline. To evaluate whether deviations in performance were a result of physical aging trends, the entire dataset was plotted in O_2/N_2 and H_2/CH_4 upper bounds, as shown in **Figure S3,** and fit to the mathematical expression of the upper bound, as described by **Eq. 11** [47,48]:

$$P = k\alpha_{ij}^{n} \tag{11}$$

The slope of the upper bound line on a log-log plot is captured by the factor *n*. As a glassy polymer ages, the decrease in permeability and increase in selectivity usually follows a trend that is parallel to the upper bound of the targeted gas pair. In this case, the slope obtained from fitting the dataset does not match the slope of the reported upper bound (**Figure S3**). Therefore, physical aging was not considered the primary factor contributing to variation in as-submitted permeabilities. Overall, however, reporting comprehensive synthetic procedures, casting protocols, as well as post-casting treatment and storage conditions are essential to maintain consistency across the membrane community.

No consideration was given as to whether or not there were batch-to-batch variations in the films purchased from the supplier (Goodfellow). Quality control could be another source of error, but this type of evaluation would be very difficult without proprietary information. Other sources of error, which are discussed below, showed co-dependencies on uncertainty, so we believe that batch-to-batch variability is not a major factor in this study.

3.3.2. Sample preparation

Once the film is cast, the thickness is often measured using a micrometer. Then, the sample is mounted on a support and the exposed membrane area is measured. Sample preparation conditions reported by the participating labs are shown in **Table S4**. Commonly used supports include Aluminum tape or brass disks and common adhesives include Devcon 5-min epoxy. Micrometers and area measurement tools include the Mitutoyo micrometer Series 293 and ImageJ software, respectively. As shown in **Table S4**, storage conditions ranged widely between participating labs, but no systematic deviations were observed between storage conditions and transport properties for the PSf samples. The reported areas used for testing ranged from 0.6 cm^2 to 6.3 cm^2, but no correlation was found between area differences and variation in the permeation for H_2 ($R^2 = 0.003$) and CH_4 ($R^2 = 0.007$), as shown in **Fig S4**. Additionally, while the thickness provided by Goodfellow was 25 μm, the self-reported thicknesses ranged from 23.6 μm to 29 μm. From **Eq. 7**, this range in thicknesses would account for a difference in reported permeabilities values of up to approximately 23%. Interestingly, a weak correlation was found between thickness and the variation in the permeation for H_2 ($R^2 = 0.134$) and CH_4 ($R^2 = 0.094$) (**Fig S4**). While these co-dependencies represented by R^2 values are small, they are the most significant co-dependencies outside of those for leak rates, which will be discussed later. Therefore, ensuring an appropriate active area and especially thickness is required for accurate testing. In all cases, storage conditions, thickness, area, and standard deviations should be reported.

3.3.3. Equipment information

Pressure transducer uncertainty, downstream volume calibration, and ensuring a tight seal of the permeation cell to achieve low leak rates can influence calculated permeabilities. **Table S5** summarizes these details for study participants, as well as information about gas suppliers and purity. Gas purity was usually over 99% for all gases and revealed no correlation with reported deviations in transport properties for both H_2 ($R^2 = 5 \times 10^{-4}$) and CH_4 ($R^2 = 0.004$). All labs except Lab 3 used an in-line stainless steel filter holder as the permeation cell.

When considering the basic components for a constant-volume variable-pressure system, errors associated with the pressure transducers and the temperature controller will add a small percentage of error to the data. The reader is referred to **Table S5** for detailed descriptions of these components used by each study participant. The upstream pressure transducers varied by provider, maximum pressure, and accuracies of 0.05% to 0.5% of the full scale of the transducer. Another source of possible error is from the zero-point offset for a transducer. However, permeabilities are calculated based on changes in downstream pressure, and not on the absolute values of pressure, so these offset uncertainties should have little to no effect on the results. Nevertheless, for the interested reader, the majority of the downstream pressure transducers used were MKS Baratron® capacitance manometers, with an accuracy ranging from 0.12% to 0.25% of the pressure reading. Because permeability calculations require a good estimate of transport rates and leak rates in the downstream of the system, it is common practice to use very sensitive downstream pressure transducers, which can be especially useful for less permeable samples where the transport rate is very low. On the other hand, zero-point offsets and span uncertainties may have a larger impact on upstream pressure transducer readings, but there were no significant dependencies between permeabilities and reported upstream pressures (**Fig. S4**).

Additionally, for most labs, the temperature was maintained using an air bath or a water bath with a Thermo Scientific™ immersion circulator, and there were little variations reported for temperature in the submitted data. For Lab 4, a heating jacket was used to heat the cell while the gases flow at ambient temperatures. Because the temperature parameter in **Eq. 7** is not defined precisely (i.e., it is not specified whether this is the temperature in the entire system or the isolated membrane), there could be some added uncertainty to permeation results. The most common arrangement involves heating of the upstream and downstream tubing as well as the cell, and deviating from this arrangement can result in calculation errors at temperatures other than ambient.

In addition to installing suitable parts on the permeation apparatus, a critical component to retain accuracy is the calibration and size of the downstream volume. If the volume is too small, the downstream pressure may rapidly exceed the limit of the downstream pressure transducer, precluding time-lag calculations. Conversely, if it is too large, extracting accurate pressure-rise data may be difficult within the transducer resolution. The size of the downstream volumes for study participants ranged from 2.86 cm^3 to 166.5 cm^3 and very weak correlations were observed between permeability and the size of the downstream volume for both H_2 ($R^2 = 0.057$) and CH_4 ($R^2 = 0.065$). Standard volume calibration procedures are summarized in **Table S6**. Calibration methods include: (1) filling the vessel with a solvent at room temperature or with very small stainless steel pellets, (2) performing a Burnett expansion with He or H_2 [49], or (3) measuring the permeability of a standard polymer (e.g., polycarbonate or Kapton) and estimating the size of the volume based on literature data. Generally, constant-volume variable-pressure systems should be calibrated during installation and when major modifications are made to the system. It is also advisable to perform volume calibrations in triplicate and report the measurement uncertainty.

3.3.4. Testing conditions

Once the sample is prepared for testing, material-dependent testing conditions must be optimized. These include (1) hold time for the test to reach steady state, (2) de-gas time for removal of ambient contaminants at the beginning of the experiment, and (3) de-gas time for removal of residual gas from a previous test. The testing conditions used for this study are summarized in **Table S7**. All labs reported a testing temperature of approximately 35 °C, with the lowest temperature reported at 34.5 °C for Lab 6 and the highest of 35.1 °C for Labs 1 and 8. De-gas times at the beginning of the experiment ranged from 1 h to 24 h.

When switching between gases, it is common to vent the residual gas, flush with an inert gas, and hold the system under vacuum for a certain amount of time before proceeding to the next gas. The de-gas time between tests of different gases should be sufficiently long to ensure that all gas has been removed from the film. In this study, most labs evacuated the permeation cell for at least 1 h before running the next test, which is over eleven times the average time-lag value estimated for CH_4. Some labs evacuated until the downstream reached a certain pressure (e.g., 2 torr for Lab 8 and 0.1 torr for Lab 1). When testing a new membrane sample, it has been previously recommended that tests should be run for at least six times of the time-lag to ensure the steady-state region is reached [19]. As shown in **Table S7**, de-gas and hold times between experiments varied widely from lab to lab. However, it was common practice for all labs to hold CH_4 and N_2 for a longer period of time than H_2 and O_2 for permeation experiments and for de-gassing. Of note, labs with self-reported time lags held the gases for at least six times their time lag, with hold times ranging from 6.8–35.7 times the time lag for CH_4 to 16.1–221 times the time lag for O_2. When time lag was not self-reported, the hold times were always found to be over six times the average time lag values reported in **Table 3**. It is also important to note that many researchers consider

lower pressure tests than those considered here (i.e., 1 bar). At lower pressures, even longer hold times and de-gas times are required because the effective diffusion coefficient and overall gas flux decreases, resulting in larger time lags [19,44,50].

A critical component in ensuring accuracy of a permeation calculation includes monitoring the leak rate of the system. A widely reported heuristic in the membrane community is to ensure that the leak rate is at least ten times lower than the transport rate (< 10%) [19]. When a sample is not permeable enough, thinner films and larger active areas are frequently prepared. Additionally, tighter cell seals can reduce the leak rate. **Table S8** summarizes the leak rates observed for the systems in this study and the strength of the seal of the cell, which was defined as the ratio of the leak rate to the downstream volume size. The tighter the seal, the better the leak rate of the system. Leak rates ranged from 1.77×10^{-7} to 8.8×10^{-5} torr s^{-1} while the strength of the seal ranged from 1.8×10^{-9} to 1.9×10^{-6} torr s^{-1} cm^{-3}. Some common practices to ensure proper tightness of the cell include greasing of the O-rings in the permeation cell and pre-heating the cell and re-tightening the system. The latter approach (i.e., heating the cell) can help to desorb atmospheric gases and vapors that may be adsorbed in the metal tubing of the systems, further reducing the effective "leak" rate. **Table S8** also presents the ratio of the steady-state transport rates versus the leak rates for CH_4. All labs had transport rates greater than ten times that of the leak rate. In other words, the leak rate was always less than 10% of the transport rate for the slowest gas. For faster permeating gases (i.e., H_2 and O_2), the leak rates were less than 1% of the transport rate. Finally, because the vacuum gauge of each apparatus will range from lab to lab, it can be helpful to monitor the minimum downstream pressure reached during a permeation test to facilitate time-lag calculations. Common values for the minimum downstream pressure are shown in **Table S8**.

3.3.5. Calculations

As shown in **Eq. 7**, many parameters can be influenced by the variability of the measurement and the subsequent permeability calculation. Error propagation is commonly used to estimate the uncertainties in system volume, temperature, pressure rise, and sample thickness and area. However, errors are often unreported, and when they are, many studies do not specify if error was calculated from error propagation or standard deviations from multiple measurements. This information would provide helpful details when evaluating work in the open literature.

Moreover, permeation calculations are not often cross-examined by multiple individuals. Taking advantage of the large dataset provided here, we re-calculate the permeation data for all labs using the submitted raw datasets. Re-calculated values were compared to the as-submitted data to provide an estimate for the "human error" associated with the estimation of the steady-state region in permeation calculations. All other parameters in **Eq. 7** were kept constant using the as-submitted data for l, V_d, A, and T. As shown in **Figure 9**, all permeability calculations remained within an error of 2.5% for almost all data points, with a few scattered data points above 4%. These results indicate that variations in the calculation of $\left[\left(\frac{dp_1}{dt}\right)_{ss} - \left(\frac{dp_1}{dt}\right)_{leak}\right]$ in **Eq. 7** alone can result in permeability differences of up to 5%.

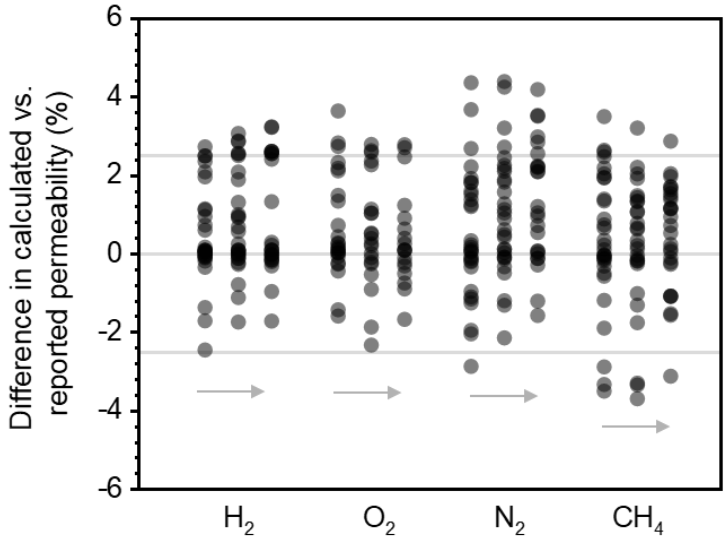

Figure 9. Difference in re-calculated versus self-reported permeabilities for PSf tested at 35 °C. Arrows represent increases in pressure.

In addition to the leak rate and transport rate, variations in l, V_d, A, and p will also contribute to the overall error in permeability data. To elucidate the varying contributions from each parameter in **Eq. 7**, the percent error contributed from each variable to the total error propagation was calculated. This analysis includes all data where non-zero uncertainties for all variables (i.e., l, V_d, A, and p) were provided. The total error propagation (%) and corresponding percentages contributed from each of the four variables are summarized in **Table S9**. Generally, the percent contributions to the overall error propagation vary widely. However, in these examples, the largest statistically significant contributor to error was from the thickness measurements of the films. Ultimately, it is important to include all parameters in **Eq. 7** in error propagation estimates, most notably uncertainties related to thickness.

Another important metric in the evaluation of gas transport properties is the time-lag calculation. One of the advantages of this method is the accessibility of diffusion data obtained directly from permeation tests. However, little is known regarding the accuracy, sensitivity, and reproducibility of such measurements. In this analysis, time lags for H_2 were not included because the reported values ranged widely in magnitude and, in certain cases, were unphysical (i.e., negative values). **Figure 10** presents as-submitted and manually re-calculated time lags, following a similar procedure to that used for the permeability analysis. For O_2 and N_2, significant deviations were found between the self-reported time-lag estimates and re-calculated values for certain labs. Of particular note, self-reported values ranged widely between labs, indicating that time lag estimates can be highly biased by the system or calculation technique. In some cases, the response time of the operator or instrument may contribute to the overall time lag calculated. To account

for this potential source of error, response times could be estimated using a barrier film with a small pinhole or a PDMS thin film with negligible time lag [51]. The time it takes between starting an experiment and reaching a stable upstream pressure can be estimates from the instantaneous pressure responde in the downstream. Notably, however, CH_4 time-lag values were consistent across labs and in re-calculations. This result suggests a much stronger reliability in measurements for slower permeating gases with longer time-scales for diffusion than for more rapidly permeating gases. As discussed previously, CH_4 is often tested last, after extensive de-gassing, and with longer hold times than for other gases. These factors can contribute to accurate time lag estimates. In terms of application, we would expect that short time lags reported in the literature, for example, for high free volume polymers, would have the most uncertainty.

In addition to overcoming fundamental challenges related to fast diffusion for certain gases, the selection of the steady-state region and the initial time point of the experiment for time-lag calculations will also bias the results and contribute to uncertainty. Performing time-lag estimates manually and plotting the resulting data at the steady state region can help to confirm accuracy and consistency of the fitting.

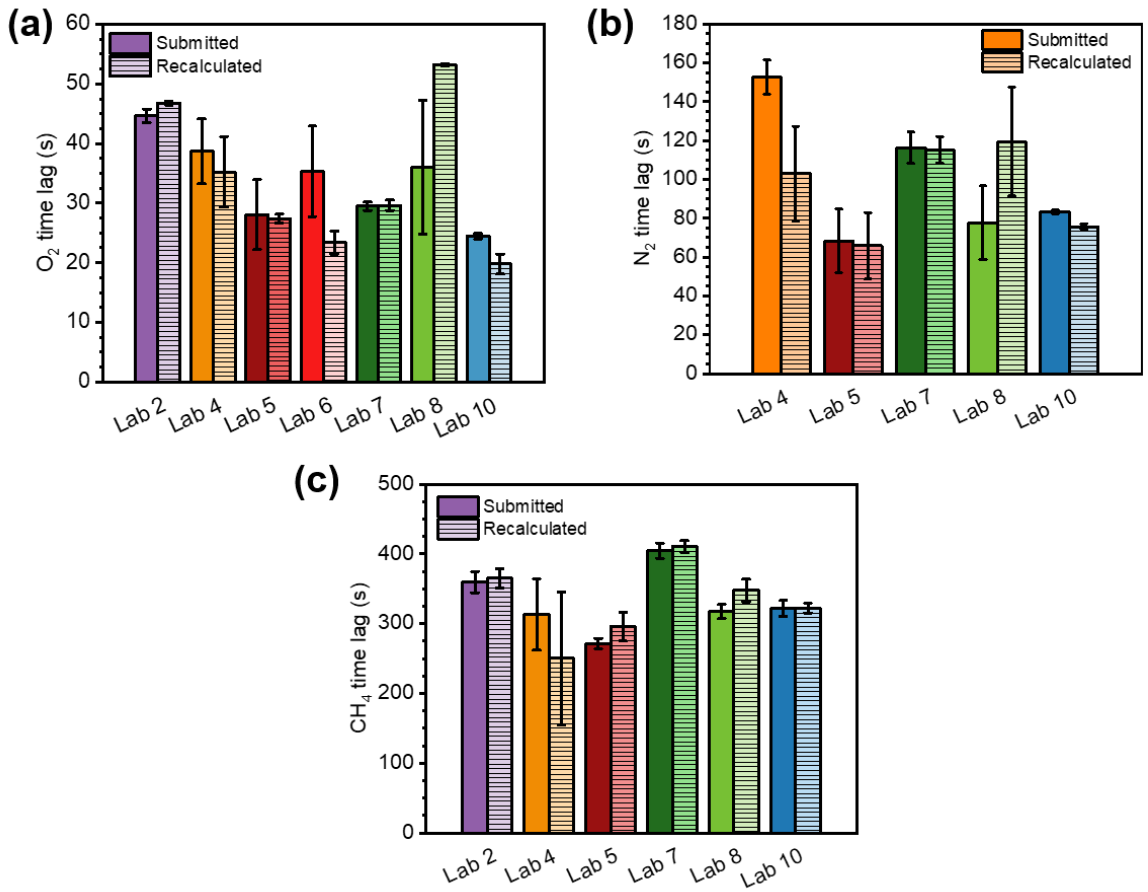

Figure 10. (a) O_2, (b) N_2, and (c) CH_4 time-lag values for PSf tested at 10 bar and 35 °C. Uncertainties indicate standard deviations from three independent measurements.

3.3.6. Recommended permeation testing protocol checklist

Here, a recommended set of steps for conducting permeation tests is provided to ensure that permeation testing is as reliable and as reproducible as possible:

Synthesis, casting, and sample preparation:

1. Ensure that solvent removal is complete and that thermal treatment conditions align with comparative literature.
2. Store the sample in a controlled environment. Record ambient temperature and humidity.

3. Measure the film thickness and active area at least three times and report the mean along with uncertainties.

Equipment information:

1. Know the specifications of the system being used including details about the pressure transducers, temperature controllers, and downstream volume size and related uncertainties. Report this information in publications.
2. Report detailed information about the method used to calculate error (e.g., error propagation or standard deviations of triplicates).
3. Report the volume calibration procedure used for the system. Confirm that no major changes have been performed to the system since the last volume calibration. If there have been major changes, re-calibrate the volume.

Testing conditions:

1. Measure the leak rate of the system and the minimum pressure of the downstream.
2. Run an initial de-gas for a sufficient time and sufficient temperature to adequately remove residual gases in the film.
3. Test the film for a long enough hold time to ensure that steady state has been reached.
4. Between gases, make sure to remove residual gas from the system by de-gassing for at least the time it took the previous gas to reach steady state.

Calculations and reporting:

1. Confirm that the steady-state region has been reached. Ensure that the leak rate is less than 10% of the steady-state transport rate.
2. Subtract the leak rate and/or minimum pressure from the data before performing calculations.

3. Perform time-lag calculations manually to view fitted and extrapolated steady-state pressure response, and if possible, test in triplicate.
4. Have multiple researchers calculate permeability and time lags independently using the raw data. Compare calculations.
5. Report a detailed procedure of the permeation testing and calculation in published work.

4. Conclusions

Constant-volume variable-pressure permeation testing is an essential technique with widespread use for assessing gas transport properties. In this work, a 10-participant multi-lab study was performed using this technique to provide a reference standard and a list of best practices for the membrane community. Data was collected for H_2, O_2, N_2, and CH_4 permeabilities for PSf at 35 °C and 10, 15, and 20 bar. Self-reported data were compared between labs and with literature to provide lab-to-lab uncertainties and acceptable ranges for permeability and time-lag calculations. Detailed equipment information, lab-specific experimental procedures, and raw data were compared and evaluated to derive a list of best practices and heuristic guidelines for conducting reliable pure-gas permeation testing. The primary source of variation in permeability was attributed to the uncertainties in sample thickness. High variability was also found in the calculation of time lag and thus the reported diffusion coefficients. In summary, this work provides a comprehensive set of guiding principles for consistent and reproducible pure-gas permeation testing and a reference standard to be used by the membrane community.

CRediT author statement

Katherine Mizrahi Rodriguez: Conceptualization, Methodology, Software, Formal Analysis, Investigation, Data Curation, Writing – Original Draft. **Wan-Ni Wu:** Formal Analysis, Software, Validation, Writing – Review and Editing. **Taliehsadat Alebrahim**: Investigation, Data Curation,

Writing – Review and Editing. **Yiming Cao**: Writing – Review and Editing, Supervision. **Benny D. Freeman**: Writing – Review and Editing, Supervision. **Daniel Harrigan**: Investigation, Data Curation, Writing – Review and Editing. **Mayank Jhalaria**: Investigation, Data Curation, Writing – Review and Editing. **Adam Kratochvil**: Investigation, Data Curation, Writing – Review and Editing. **Sanat Kumar**: Writing – Review and Editing, Supervision. **Won Hee Lee**: Investigation, Data Curation, Writing – Review and Editing. **Young Moo Lee**: Writing – Review and Editing, Supervision. **Haiqing Lin**: Writing – Review and Editing, Supervision. **Lina Wang**: Investigation, Data Curation, Writing – Review and Editing. **Julian M. Richardson** : Investigation, Data Curation, Writing – Review and Editing. **Qilei Song**: Writing – Review and Editing, Supervision. **Benjamin Sundell**: Investigation, Data Curation, Writing – Review and Editing. **Raymond Thür**: Investigation, Data Curation, Writing – Review and Editing. **Ivo Vankelecom**: Writing – Review and Editing, Supervision. **Anqi Wang**: Investigation, Data Curation, Writing – Review and Editing. **Catherine Wiscount**: Investigation, Data Curation, Writing – Review and Editing. **Zachary P. Smith:** Conceptualization, Writing – Review and Editing, Supervision.

Declaration of competing interest

The authors have no known competing financial interests or personal relationships that could influence the work reported in this paper.

Acknowledgements

This work was supported by the U.S. Department of Energy, Office of Science, Office of Basic Energy Sciences, Separation Science program (award number: DE-SC0019087). K.M.R. acknowledges support from an NSF-GRFP fellowship (DGE-1122374). W.W. also acknowledges support from the T.S. Lin fellowship. T.A. and H.L. acknowledge support from National Science Foundation (award number: 1554236). Y.M.L. acknowledges the financial support from the

National Research Foundation of Korea (NRF) funded by the Ministry of Science and ICT (NRF-2018M1A2A2061979) and by the Material Component Technology Development (20010955) through the Korea Evaluation Institute of Industrial Technology (KEIT) funded by the Ministry of Trade, Industry, and Energy, Republic of Korea. Y.M. Cao and L.W. acknowledge support from the Chinese academy of sciences (COMS2019J09, DNL180202 & DICPI202010). J.M.R. and B.D.F.'s contributions to this study were supported by the U.S. Department of Energy, Office of Science, Office of Basic Energy Sciences under Award Number DE-FG02-02ER15362. S.K. acknowledges financial support for this research from the Department of Energy under grant DE-SC0021272. A.W. and Q.S. acknowledge support from UK EPSRC (SynHiSel, EP/V047078/1).

Appendix A. Supplementary data

Supplementary data to this article can be found online.

References

[1] B. Comesaña-Gándara, J. Chen, C.G. Bezzu, M. Carta, I. Rose, M.C. Ferrari, E. Esposito, A. Fuoco, J.C. Jansen, N.B. McKeown, Redefining the Robeson upper bounds for CO_2/CH_4 and CO_2/N_2 separations using a series of ultrapermeable benzotriptycene-based polymers of intrinsic microporosity, Energy Environ. Sci. 12 (2019) 2733–2740. https://doi.org/10.1039/c9ee01384a.

[2] Q. Qian, P.A. Asinger, M.J. Lee, G. Han, K. Mizrahi Rodriguez, S. Lin, F.M. Benedetti, A.X. Wu, W.S. Chi, Z.P. Smith, MOF-Based Membranes for Gas Separations, Chem. Rev. 120 (2020) 8161–8266. https://doi.org/10.1021/acs.chemrev.0c00119.

[3] W.H. Lee, J.G. Seong, X. Hu, Y.M. Lee, Recent progress in microporous polymers from

thermally rearranged polymers and polymers of intrinsic microporosity for membrane gas separation: Pushing performance limits and revisiting trade-off lines, J. Polym. Sci. 58 (2020) 2450–2466. https://doi.org/10.1002/pol.20200110.

[4] R. Swaidan, B. Ghanem, E. Litwiller, I. Pinnau, Physical Aging, Plasticization and Their Effects on Gas Permeation in “rigid” Polymers of Intrinsic Microporosity, Macromolecules. 48 (2015) 6553–6561. https://doi.org/10.1021/acs.macromol.5b01581.

[5] M. McNutt, Reproducibility, Science . 343 (2014) 229. https://doi.org/10.1126/science.1250475.

[6] M. Baker, D. Penny, Is there a reproducibility crisis?, Nature. 533 (2016) 452–454. https://doi.org/10.1038/533452A.

[7] R. Han, K.S. Walton, D.S. Sholl, Does chemical engineering research have a reproducibility problem?, Annu. Rev. Chem. Biomol. Eng. 10 (2019) 43–57. https://doi.org/10.1146/annurev-chembioeng-060718-030323.

[8] E. Guen, P. Klapetek, R. Puttock, B. Hay, A. Allard, T. Maxwell, P.O. Chapuis, D. Renahy, G. Davee, M. Valtr, J. Martinek, O. Kazakova, S. Gomès, SThM-based local thermomechanical analysis: Measurement intercomparison and uncertainty analysis, Int. J. Therm. Sci. 156 (2020) 106502. https://doi.org/10.1016/j.ijthermalsci.2020.106502.

[9] J.P.A. Ioannidis, Why most published research findings are false, PLoS Medicine. 2(8) (2005). https://doi.org/10.1371/journal.pmed.0020124.

[10] C.G. Begley, L.M. Ellis, Drug development: Raise standards for preclinical cancer research, Nature. 483 (2012) 531–533. https://doi.org/10.1038/483531a.

[11] J.P.A. Ioannidis, S. Greenland, M.A. Hlatky, M.J. Khoury, M.R. Macleod, D. Moher, K.F. Schulz, R. Tibshirani, Increasing value and reducing waste in research design, conduct, and analysis, Lancet. 383 (2014) 166–175. https://doi.org/10.1016/S0140-6736(13)62227-8.

[12] M. Agrawal, R. Han, D. Herath, D.S. Sholl, Does repeat synthesis in materials chemistry obey a power law?, Proc. Natl. Acad. Sci. U. S. A. 117 (2020) 877–882. https://doi.org/10.1073/pnas.1918484117.

[13] J. Park, J.D. Howe, D.S. Sholl, How Reproducible Are Isotherm Measurements in Metal-Organic Frameworks?, Chem. Mater. 29 (2017) 10487–10495. https://doi.org/10.1021/acs.chemmater.7b04287.

[14] D.S. Sholl, Five Easy Ways to Make Your Research More Reproducible, Langmuir. 35 (2019) 13257–13258. https://doi.org/10.1021/acs.langmuir.9b02963.

[15] H.G.T. Nguyen, L. Espinal, R.D. van Zee, M. Thommes, B. Toman, M.S.L. Hudson, E. Mangano, S. Brandani, D.P. Broom, M.J. Benham, K. Cychosz, P. Bertier, F. Yang, B.M. Krooss, R.L. Siegelman, M. Hakuman, K. Nakai, A.D. Ebner, L. Erden, J.A. Ritter, A. Moran, O. Talu, Y. Huang, K.S. Walton, P. Billemont, G. De Weireld, A reference high-pressure CO_2 adsorption isotherm for ammonium ZSM-5 zeolite: results of an interlaboratory study, Adsorption. 24 (2018) 531–539. https://doi.org/10.1007/s10450-018-9958-x.

[16] T.Y. Cath, M. Elimelech, J.R. McCutcheon, R.L. McGinnis, A. Achilli, D. Anastasio, A.R. Brady, A.E. Childress, I. V. Farr, N.T. Hancock, J. Lampi, L.D. Nghiem, M. Xie, N.Y. Yip, Standard Methodology for Evaluating Membrane Performance in Osmotically

Driven Membrane Processes, Desalination. 312 (2013) 31–38. https://doi.org/10.1016/j.desal.2012.07.005.

[17] D.S. Sholl, R.P. Lively, Exemplar Mixtures for Studying Complex Mixture Effects in Practical Chemical Separations, JACS Au. 2 (2022) 322-327. https://doi.org/10.1021/jacsau.1c00490.

[18] A Research Agenda for Transforming Separation Science, National Academies Press, Washington, D.C., (2019). https://doi.org/10.17226/25421.

[19] H. Lin, B.D. Freeman, Permeation and Diffusion, Springer Handb. Mater. Meas. Methods. (2006) 371–387.

[20] A. Drews, Standard Test Method for Determining Gas Permeability Characteristics of Plastic Film and Sheeting, ASTM Int. D1434-e1 (2009). https://standards.globalspec.com/std/9958461/ASTM D1434 (accessed July 16, 2021).

[21] J.G. Wijmans, R.W. Baker, The solution-diffusion model: a review, J. Membr. Sci. 107 (1995) 1–21. https://doi.org/10.1016/0376-7388(95)00102-I.

[22] S. Matteucci, Y. Yampolskii, B.D. Freeman, I. Pinnau, Transport of Gases and Vapors in Glassy and Rubbery Polymers, Mater. Sci. Membr. Gas Vap. Sep. (2006) 1–47. https://doi.org/10.1002/047002903X.ch1.

[23] D.R. Paul, Gas Sorption and Transport in Glassy Polymers., Berichte Der Bunsengesellschaft/Physical Chem. Chem. Phys. 83 (1979) 294–302. https://doi.org/10.1002/bbpc.19790830403.

[24] J.W. Westwater, H.G. Drickamer, The Mathematics of Diffusion, 1957.

https://doi.org/10.1021/ja01562a072.

[25] R.M. Barrer, E.K. Rideal, Permeation, diffusion and solution of gases in organic polymers, Trans. Faraday Soc. 35 (1939) 628–643. https://doi.org/10.1039/tf9393500628.

[26] H.A. Daynes, The process of diffusion through a rubber membrane, Proc. R. Soc. Lond. A. 97 (1920) 286–307. https://doi.org/10.1098/rspa.1920.0034.

[27] C.M. Zimmerman, A. Singh, W.J. Koros, Diffusion in gas separation membrane materials: A comparison and analysis of experimental characterization techniques, J. Polym. Sci. Part B Polym. Phys. 36 (1998) 1747–1755. https://doi.org/10.1002/1099-0488(19980730)36:10;2-9.

[28] H.L. Frisch, The time lag in diffusion, J. Phys. Chem. 61 (1957) 93–95. https://doi.org/10.1021/j150547a018.

[29] Polysulfone Film - online catalog source - supplier of research materials in small quantities - Goodfellow. http://www.goodfellow.com/A/Polysulfone-Film.html (accessed September 30, 2021).

[30] N.K. Mishra, N. Patil, M. Anas, X. Zhao, B.A. Wilhite, M.J. Green, Highly selective laser-induced graphene (LIG)/polysulfone composite membrane for hydrogen purification, Appl. Mater. Today. 22 (2021) 100971. https://doi.org/10.1016/j.apmt.2021.100971.

[31] Y. Huang, D.R. Paul, Physical aging of thin glassy polymer films monitored by gas permeability, Polymer. 45 (2004) 8377–8393. https://doi.org/10.1016/j.polymer.2004.10.019.

[32] S. Neumann, G. Bengtson, D. Meis, V. Filiz, Thermal Cross Linking of Novel Azide

Modified Polymers of Intrinsic Microporosity—Effect of Distribution and the Gas Separation Performance, Polymers (Basel). 11 (2019) 1241. https://doi.org/10.3390/polym11081241.

[33] P. Mishra, C. Pandey, U. Singh, A. Gupta, C. Sahu, A. Keshri, Descriptive statistics and normality tests for statistical data, Ann. Card. Anaesth. 22 (2019) 67. https://doi.org/10.4103/aca.ACA_157_18.

[34] A.B. Foster, M. Tamaddondar, J.M. Luque-Alled, W.J. Harrison, Z. Li, P. Gorgojo, P.M. Budd, Understanding the Topology of the Polymer of Intrinsic Microporosity PIM-1: Cyclics, Tadpoles, and Network Structures and Their Impact on Membrane Performance, Macromolecules. 53 (2020) 569–583. https://doi.org/10.1021/acs.macromol.9b02185.

[35] R.R. Tiwari, J. Jin, B.D. Freeman, D.R. Paul, Physical aging, CO_2 sorption and plasticization in thin films of polymer with intrinsic microporosity (PIM-1), J. Membr. Sci. 537 (2017) 362–371. https://doi.org/10.1016/j.memsci.2017.04.069.

[36] R.R. Tiwari, Z.P. Smith, H. Lin, B.D. Freeman, D.R. Paul, Gas permeation in thin films of "high free-volume" glassy perfluoropolymers: Part I. Physical aging, Polymer. 55 (2014) 5788–5800. https://doi.org/10.1016/j.polymer.2014.09.022.

[37] L. Shao, T.S. Chung, G. Wensley, S.H. Goh, K.P. Pramoda, Casting solvent effects on morphologies, gas transport properties of a novel 6FDA/PMDA-TMMDA copolyimide membrane and its derived carbon membranes, J. Membr. Sci. 244 (2004) 77–87. https://doi.org/10.1016/j.memsci.2004.07.005.

[38] B.W. Rowe, B.D. Freeman, D.R. Paul, Influence of previous history on physical aging in thin glassy polymer films as gas separation membranes, Polymer. 51 (2010) 3784–3792.

https://doi.org/10.1016/j.polymer.2010.06.004.

[39] M.R. Khdhayyer, E. Esposito, A. Fuoco, M. Monteleone, L. Giorno, J.C. Jansen, M.P. Attfield, P.M. Budd, Mixed matrix membranes based on UiO-66 MOFs in the polymer of intrinsic microporosity PIM-1, Sep. Purif. Technol. 173 (2017) 304–313. https://doi.org/10.1016/j.seppur.2016.09.036.

[40] L.E. Starannikova, A.Y. Alentiev, R.Y. Nikiforov, I.I. Ponomarev, I. V. Blagodatskikh, A.Y. Nikolaev, V.P. Shantarovich, Y.P. Yampolskii, Effects of different treatments of films of PIM-1 on its gas permeation parameters and free volume, Polymer. 212 (2021) 123271. https://doi.org/10.1016/j.polymer.2020.123271.

[41] M.L. Jue, C.S. McKay, B.A. McCool, M.G. Finn, R.P. Lively, Effect of Nonsolvent Treatments on the Microstructure of PIM-1, Macromolecules. 48 (2015) 5780–5790. https://doi.org/10.1021/acs.macromol.5b01507.

[42] Z.X. Low, P.M. Budd, N.B. McKeown, D.A. Patterson, Gas Permeation Properties, Physical Aging, and Its Mitigation in High Free Volume Glassy Polymers, Chem. Rev. 118 (2018) 5871–5911. https://doi.org/10.1021/acs.chemrev.7b00629.

[43] J.S. McHattie, W.J. Koros, D.R. Paul, Gas transport properties of polysulphones: 1. Role of symmetry of methyl group placement on bisphenol rings, Polymer. 32 (1991) 840–850. https://doi.org/10.1016/0032-3861(91)90508-G.

[44] A.J. Erb, D.R. Paul, Gas sorption and transport in polysulfone, J. Membr. Sci. 8 (1981) 11–22. https://doi.org/10.1016/S0376-7388(00)82135-3.

[45] D. Nasirian, I. Salahshoori, M. Sadeghi, N. Rashidi, M. Hassanzadeganroudsari,

Investigation of the gas permeability properties from polysulfone/polyethylene glycol composite membrane, Polym. Bull. 77 (2020) 5529–5552. https://doi.org/10.1007/s00289-019-03031-3.

[46] K. Ghosal, R.T. Chern, B.D. Freeman, R. Savariar, The effect of aryl nitration on gas sorption and permeation in polysulfone, J. Polym. Sci. Part B Polym. Phys. 33 (1995) 657–666. https://doi.org/10.1002/polb.1995.090330415.

[47] L.M. Robeson, The upper bound revisited, J. Membr. Sci. 320 (2008) 390–400. https://doi.org/10.1016/j.memsci.2008.04.030.

[48] L.M. Robeson, Correlation of separation factor versus permeability for polymeric membranes, J. Membr. Sci. 62 (1991) 165–185. https://doi.org/10.1016/0376-7388(91)80060-J.

[49] E.S. Burnett, Compressibility Determinations Without Volume Measurements, J. Appl. Mech. 3 (1936) A136–A140. https://doi.org/10.1115/1.4008721.

[50] D.R. Paul, W.J. Koros, Effect of Partially Immobilizing Sorption on Permeability and the Diffusion Time Lag., J Polym Sci Part A-2 Polym Phys. 14 (1976) 675–685. https://doi.org/10.1002/pol.1976.180140409.

[51] S.C. Fraga, M. Monteleone, M. Lanč, E. Esposito, A. Fuoco, L. Giorno, K. Pilnáček, K. Friess, M. Carta, N.B. McKeown, P. Izák, Z. Petrusová, J.G. Crespo, C. Brazinha, J.C. Jansen, A novel time lag method for the analysis of mixed gas diffusion in polymeric membranes by on-line mass spectrometry: Method development and validation, J. Membr. Sci. 561 (2018) 39–58. https://doi.org/10.1016/j.memsci.2018.04.029.

1